STUDIES OF PHASE TRANSFORMATIONS IN DUCTILE IRON WITH ADDITIONS OF Ni, Cu, Mo

MRZYGŁÓD Barbara, OLEJARCZYK-WOŻEŃSKA Izabela, ADRIAN Henryk, GŁOWACKI Mirosław

AGH University of Science and Technology in Cracow, Poland, EU, mrzyglod@agh.edu.pl

Abstract

The paper presents the results of microstructure examinations of ductile iron with the additions of Ni, Cu and Mo. TTT diagrams - illustrating the range of phase stability as a function of the time of isothermal annealing at a given temperature, and CCT diagrams - illustrating the range of phase stability during continuous cooling at a predetermined rate were developed.

Keywords: Ductile iron, ADI, phase transformations, CCT diagram, TTT diagram

1. INTRODUCTION

The essence and purpose of the heat treatment of ductile iron is to rebuild its starting structure, usually based on a pearlitic matrix, and obtain cast iron with an ausferritic matrix. The type of the obtained microstructure depends to a great extent on the chemical composition of base cast iron (ductile iron in this case) and on the appropriately chosen values of heat treatment parameters. Yet, proper heat treatment of iron alloys requires good knowledge of the undercooled austenite transformations, which occurs during both continuous (anisothermal) cooling and holding at constant temperature (isothermal cooling). These data are provided by the graphs describing the phase transformations, commonly known as TTT (Time-Temperature-Transformation) or CCT (Continuous Cooling Transformations) diagrams, plotted in the temperature-time coordinate system. It needs to be emphasized, however, that, while in the case of steel an extensive collection of such diagrams is readily available [1], for cast iron such diagrams are rather scarce, mainly because only some of the cast iron grades are subjected to heat treatment. Examples of TTT diagrams for ductile iron can be found in [2-4]. This paper presents the results of microstructure examinations of ductile iron with the additions of Ni, Cu and Mo, including also the description of two important diagrams, i.e. TTT - illustrating the range of phase stability as a function of the time of isothermal annealing at a given temperature, and CCT - illustrating the range of phase stability during continuous cooling at a predetermined rate.

The CCT and TTT diagrams developed for the tested cast iron greatly enrich our knowledge about the phase transformations that occur during heat treatment of ductile iron. They also prove useful in computer modeling of these processes. Computer simulations allow a new mathematical model to recreate the course of industrial processes and analysis of the characteristics of the materials tested in a manner analogous to a real process. Computer techniques that are currently cheap and effective way to optimize, are used for modeling and analysis of phenomena occurring in many areas of research [5-10].

2. TEST MATERIAL

Tests were carried out on ductile iron of the chemical composition given in **Table 1**.

Table 1 Chemical composition of the examined cast iron

Chemical composition, %								
C	Si	Mn	P	S	Mg	Ni	Cu	Mo
3.57	2.13	0.26	0.06	0.015	0.038	1.2	0.7	0.2

Melting was carried out in a medium frequency induction furnace supplied by RADYNE with a 100 kg capacity crucible and an inert lining. The spheroidizing treatment of cast iron was performed by Sandwich process. The treatment was carried out in a slender ladle at 1400°C. From thus obtained ductile iron, ingots were cast according to EN 1564.

3. RESEARCH METHODOLOGY

3.1. Dilatometric tests

Tests were carried out using a RITA L78 LINSEIS high speed quenching dilatometer. The device is intended for dilatometric studies of metals and their alloys conducted in a wide range of the heating / cooling rates (0.01 - 150 K / s) in the temperature range from 20 to 1600°C. Due to induction heating (cooling) of the samples, temperature changes affect only the sample tested and not its environment. Accurate temperature measurement is obtained using a K-type thermocouple welded to the sample. It is possible to implement testing in vacuum (maximum vacuum of 10-5 mbar) or standard testing in a protective atmosphere of helium, the injection of which allows obtaining maximum cooling rate.For dilatometric tests 22 samples of ductile iron with ϕ3x10 dimensions were cut out.

CCT diagrams were plotted from the dilatometric curves obtained for different constant cooling rates of samples from the austenitizing temperature to ambient temperature. Cooling rates in the range from 2 to 6000 K/min were applied. The analysis was based on the determination of the starting and ending temperature points of phase transformations occurring as a result of non-isothermal decomposition of austenite. After each measurement, on the faces of the sample, two measurements of the hardness HV30 were taken. Selected samples after the dilatometric tests were subjected to metallographic examinations for a qualitative assessment of the matrix microstructure.

The TTT diagram was based on the isothermal dilatometric curves obtained for various constant temperature values of the isothermal transformation using high-speed (150 K/s) cooling of the samples from the austenitizing temperature to the temperature of isothermal transformation. The analysis was based on the determination of time-related points of the start and end of the transformation under isothermal conditions, plotting them next onto the TTT diagram. The study was conducted within the temperature range of isothermal holding from 700 to 280°C.

3.2. Microstructure examinations

Microscopic examinations and photographs of microstructure were taken on metallographic sections using an AXIO OBSERVER Z1m metallographic microscope. The following conditions of the examinations were observed:

- Specimens used for plotting of the CCT diagram were selectively etched in a 10 % aqueous solution of sodium metabisulphite $Na_2S_2O_5$. Randomly, to verify the evaluation of microstructural components etched in the above mentioned reagent, selected samples were cooled at a rate of 600 and 1800 K/min and etched in a 4 % picral according to PN-61/H-04503; picral etches bainite leaving martensite untouched.
- Specimens used for plotting of the TTT diagram were etched in nital (4% HNO_3 solution in C_2H_5OH).

4. TEST RESULTS

4.1. Determination of the critical temperatures Ac1p and Ac,k

Preliminary dilatometric measurements to determine the critical temperatures A_{c1p} and A_{c1k} were taken on a sample preheated at a rate of v = 5 K/min in the temperature range of 20-1000°C. The calculated temperatures

of A_{c1p} and A_{c1k} were equal to 755 and 851°C, respectively. In further studies, to develop the TTT and CCT diagrams, samples were austenitized at a temperature of 900°C for a period of 30 minutes.

4.2. CCT diagrams and analysis of microstructure

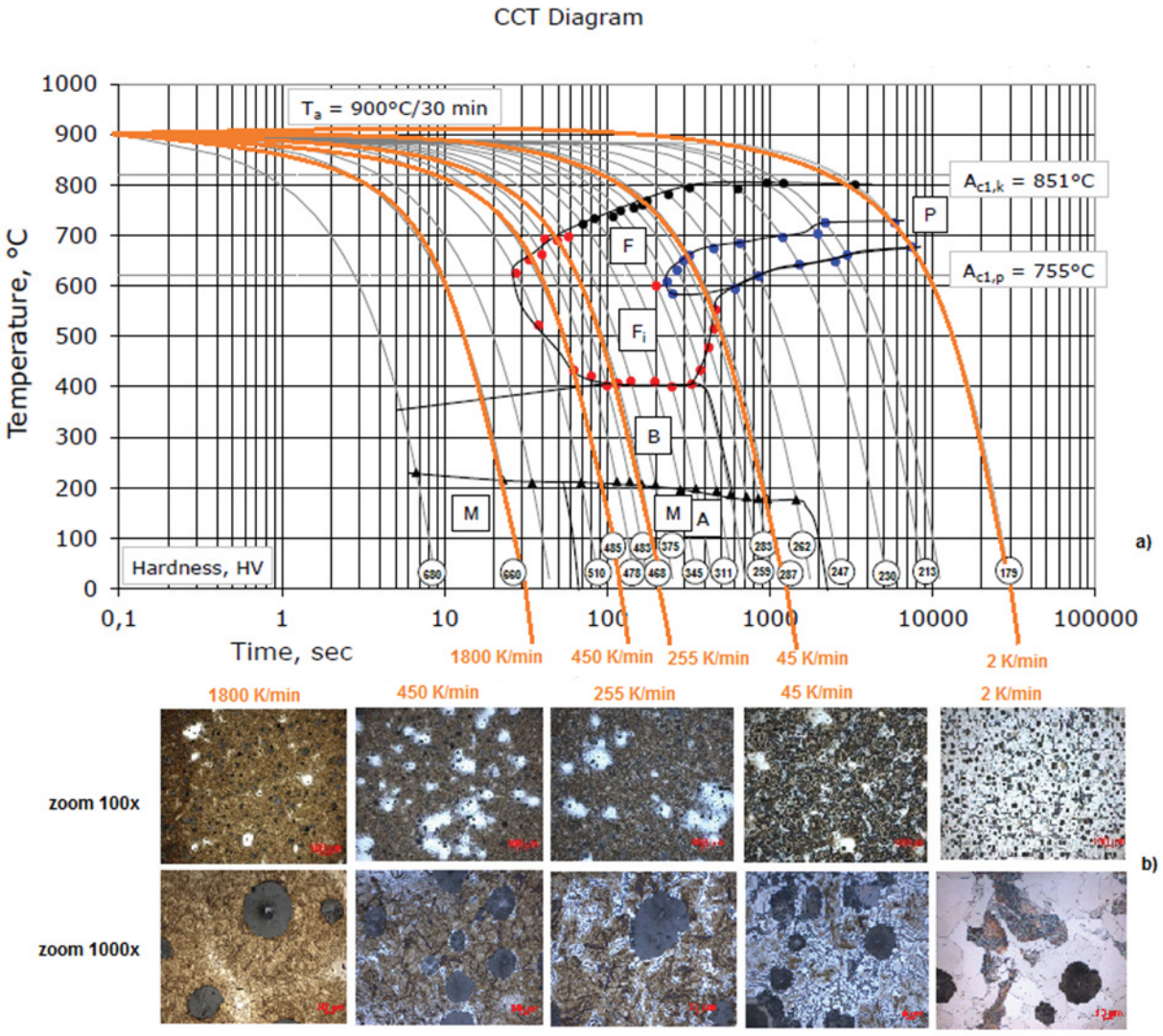

Fig. 1 CCT diagram of the examined alloy (a) and examples of microstructures (b)

The effect of cooling rate on the hardness of the tested samples is plotted in **Fig. 2**. Hardness of the samples cooled at different rates was comprised in the range of 179-680 HV. **Fig. 1** shows a CCT diagram plotted for the tested alloy. In the graph are marked temperature ranges of individual phase transformations of the undercooled

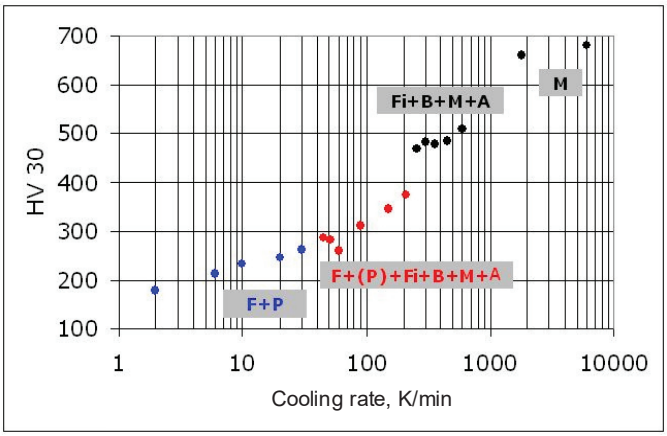

Fig. 2 Hardness HV30 and qualitative assessment of the matrix structure in selected samples cooled at different rates. B - bainite, M - martensite, A - austenite, F - pearlite, F -ferrite

austenite, i.e. austenite - ferrite, austenite - pearlite, austenite - bainite, austenite - martensite. The cooling curves of samples are also included. Each curve is provided with information about the obtained hardness value.

For the, highlighted on a CCT diagram, cooling rates of 1800, 450, 255, 45, 2 K/min, examples of the obtained microstructures are shown at magnifications of 100 and 1000X. At the lowest cooling rate of 2 K / min, the microstructure of the matrix consists of a mixture of ferrite and pearlite inside which particles of the spheroidal graphite are distributed. Ferrite content in the matrix is much larger than that of pearlite. With an increase in the rate of cooling, the microstructure of the matrix changes - the content of bainite and martensite is growing. At a cooling rate of 1800 K / min, the microstructure of the matrix comprises a mixture of bainite and martensite.

4.3. TTT diagram and microstructure analysis

A TTT diagram developed for the tested cast iron is shown in **Fig. 3**. The temperature of the austenite-bainite transformation is comprised in the range of 550 °C - Ms. The TTT diagram shows two ranges of the austenite-bainite transformation, the first one of 550 - 360 ºC (upper bainite) and the second one of 360 ºC- Ms (lower bainite). The temperature of the start of martensite transformation is 200°C, and slightly decreases with time. At a temperature above 550 °C, the austenite-pearlite transformation begins. Analysis of the resulting graph shows that with the increase in austempering temperature, the rate of bainite transformation increases, while the incubation period of transformation decreases. From the TTT diagram it also follows that the temperature of the maximum rate of austenite-to-pearlite transformation is approx. 615 ºC. The incubation period for the transformation of pearlite is approx. 120 seconds, while the incubation period for the transformation of austenite to upper bainite - at 550 °C - is approx. 100 seconds. In contrast, the incubation period for the transformation of austenite to lower bainite - at 280 °C - is approx. 450 seconds. The end of pearlite transformation at a temperature of 550°C takes place after 600 seconds, the end of bainite transformation at a temperature of 350°C after 75 minutes, and of bainite transformation at 280 °C after approx. 2 hours. The microstructure of the matrix of the tested cast iron after heat treatment in the range of 550 ºC - Ms is a mixture of bainite and austenite. It can be observed that as the temperature of the isothermal transformation increases, the length of the needles of bainitic ferrite is increasing, too.

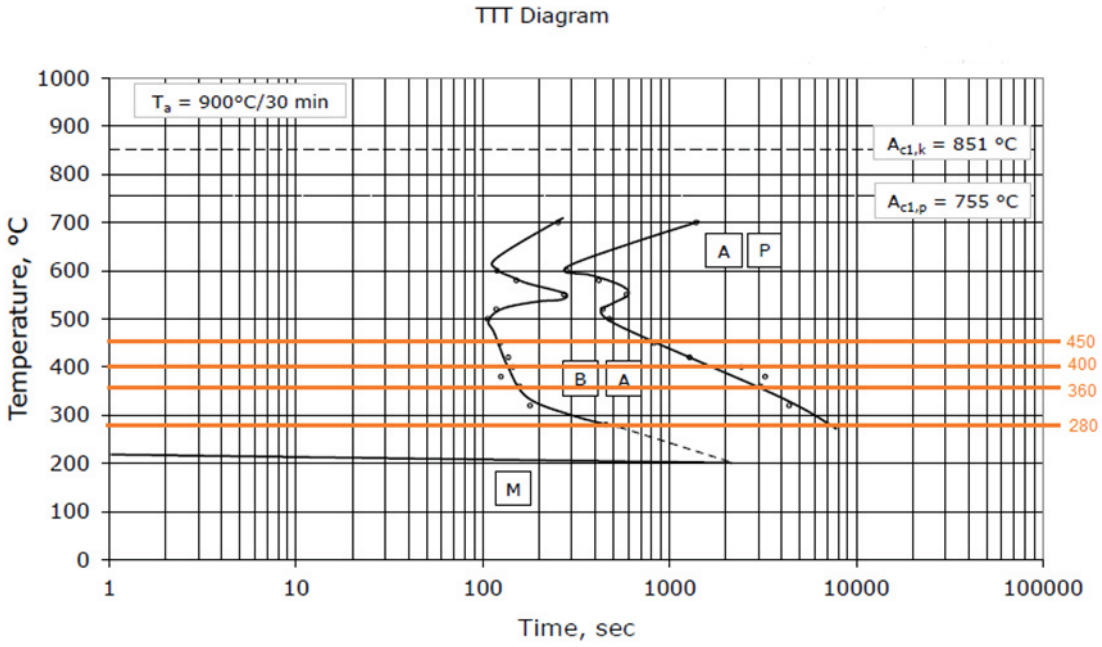

Fig. 3 TTT diagram of the examined alloy

Selected samples after isothermal dilatometric tests were subjected to metallographic examinations to evaluate the matrix microstructure. Examples of microstructures obtained at different temperatures of the isothermal transformation are shown in **Fig. 4**.

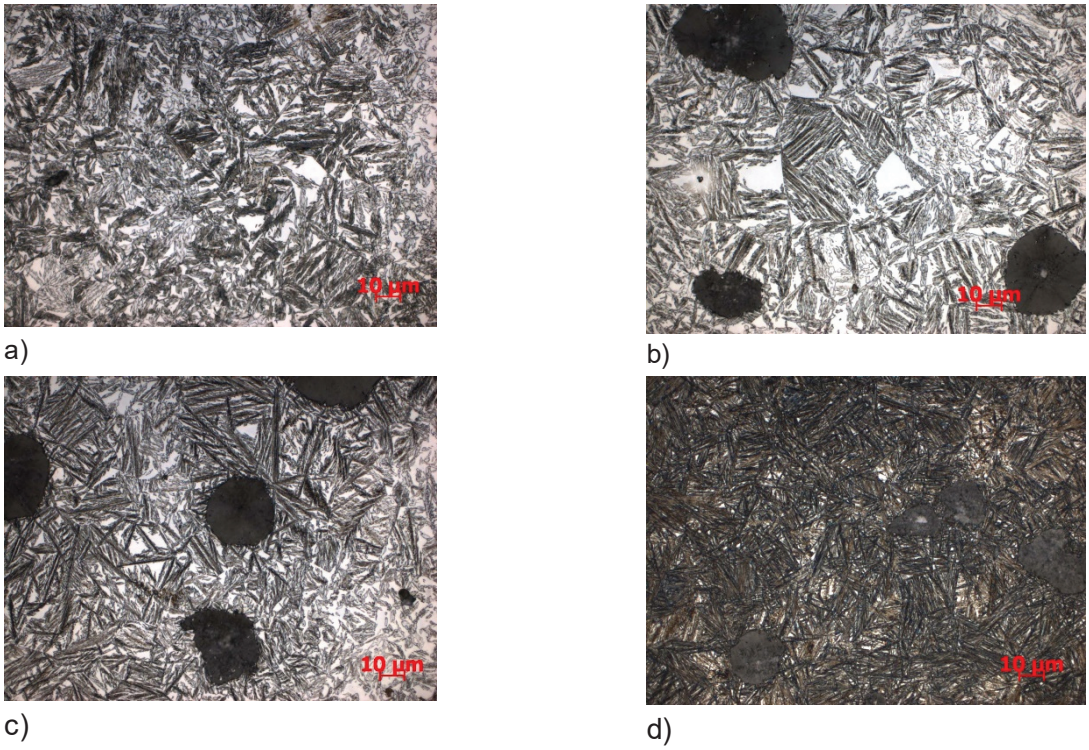

a) b) c) d)

Fig. 4 Microstructure of samples subjected to isothermal holding at the following temperatures: a) 450, b) 400, c) 360, d) 280; metallographic sections etched with Mi1Fe; 1000x

The cast iron microstructure consists of a matrix, which is a mixture of acicular ferrite and austenite, with particles of the spheroidal graphite randomly distributed in this matrix.

5. SUMMARY

Predicting the iron alloys microstructure after heat treatment is done with the help of graphs, which show the kinetics of phase transformations of the undercooled austenite under the conditions of continuous cooling (CCT diagram) or isothermal cooling (TTT diagram). Both these diagrams are an important tool aiding the design of the heat treatment processes, to ensure the achievement of the desired microstructure and mechanical properties. The paper presents the CCT and TTT diagrams plotted for ductile iron containing the additions of Ni, Cu and Mo.

The CCT diagram depicts the full range of the undercooled austenite transformation. The diffusion-induced transformations (austenite-ferrite and austenite-pearlite) occur in the temperature range of 800-400°C, bainite transformation - in the range of 400°C - Ms. The hardness of alloy subjected to continuous cooling strongly depends on the cooling rate and is comprised in the range of 179-700 HV30. The plotted TTT diagram covers the temperature range of 700-200°C. The chart clearly shows the division between the diffusion-induced transformations and bainite transformation. This chart can also be useful in the production of machine parts from ductile iron subjected to austempering heat treatment, commonly known in the literature as ADI. This cast iron is characterized by a very good combination of mechanical and plastic properties and is increasingly used in the production of selected structural components.

ACKNOWLEDGEMENTS

The study was financed under AGH Project No. 11.11.110.300

REFERENCES

[1] W. Luty, Poradnik inżyniera. Obróbka cieplna stopów żelaza. WNT, Warszawa 1977.

[2] Tybulczuk J., Kowalski A.: Żeliwo ADI - własności i zastosowanie w przemyśle, Wyd. Instytut Odlewnictwa, Kraków 2003.

[3] Özcan A., Master Thesis, The Middle East Technical University, Ankara 2003

[4] B. Mrzygłód, S. Kluska-Nawarecka, A. Kowalski, D. Wilk-Kołodziejczyk, Application of TTT diagrams of low-alloy ductile iron to assist the manufacturing process of cast iron. Transactions of Foundry Research Institute, vol. LIII, No 4, 2013, pp. 86-111.

[5] OLEJARCZYK-WOZENSKA, I.; ADRIAN, A.; ADRIAN, H.; et al. Parametric representation of TTT diagrams of ADI cast iron, Archives of Metallurgy and Materials, Vol. 57 Issue: 2, 2012, pp: 613-617.

[6] OLEJARCZYK-WOZENSKA, I.; ADRIAN, H.; MRZYGLOD, B. Mathematical model of the process of pearlite austenitization. Archives of Metallurgy and Materials, Vol. 59, Issue: 3, 2014, pp: 981-986.

[7] OLEJARCZYK, I.; ADRIAN, A.; ADRIAN, H, et al. Algorithm for controling of quench hardening process of constructional steels, Archives of Metallurgy and Materials, Vol. 55 Issue: 1, 2010, pp: 171-179.

[8] KLUSKA-NAWARECKA, S.; NAWARECKI, E.; SNIEZYNSKI, B.; et al., The recommendation system knowledge representation and reasoning procedures under uncertainty for metal casting, METALURGIJA, Vol.54, Issue:1, 2015, pp. 263-266.

[9] KLUSKA-NAWARECKA S., WILK-KOŁODZIEJCZYK D., DAJDA J., MACURA M., REGULSKI K., Computer-assisted integration of knowledge in the context of identification of the causes of defects in castings, Archives of Metallurgy and Materials, vol. 59 iss. 2/2014, pp. 743-746.

[10] WOZNIAK, D.; GLOWACKI, M.; HOJNY, M.; et al., Application of cae systems in forming of drawpieces with use rubber-pad forming processes, Archives Of Metallurgy And Materials, vol. 57 Issue 4, 2012, pp: 1179-1187.